WILEY | Hindawi

Research Article

A Study on the CO_2-Enhanced Water Recovery Efficiency and Reservoir Pressure Control Strategies

Zhijie Yang [iD],[1] Tianfu Xu [iD],[1] Fugang Wang [iD],[1] Yujie Diao [iD],[2] Xufeng Li,[2] Xin Ma,[2] and Hailong Tian [iD][1]

[1]*Key Laboratory of Groundwater Resources and Environment, Ministry of Education, Jilin University, Changchun, Jilin Province 130021, China*
[2]*Key Laboratory of Carbon Dioxide Geological Storage, Center for Hydrogeology and Environmental Geology Survey, China Geological Survey, Baoding, Hebei Province 071051, China*

Correspondence should be addressed to Fugang Wang; wangfugang@jlu.edu.cn

CO_2 geological storage (CGS) proved to be an effective way to mitigate greenhouse gas emissions, and CO_2-enhanced water recovery (CO_2-EWR) technology may improve the efficiency of CO_2 injection and saline water production with potential economic value as a means of storing CO_2 and supplying cooling water to power plants. Moreover, the continuous injection of CO_2 may cause a sharp increase for pressure in the reservoir system, so it is important to determine reasonable reservoir pressure control strategies to ensure the safety of the CGS project. Based upon the typical formation parameters of the China Geological Survey CO_2-EWR test site in the eastern Junggar Basin, a series of three-dimensional (3D) injection-extraction models with fully coupled wellbores and reservoirs were established to evaluate the effect of the number of production wells and the well spacing on the enhanced efficiency of CO_2 storage and saline production. The optimal key parameters that control reservoir pressure evolution over time are determined. The numerical results show that a smaller spacing between injection and production wells and a larger number of production wells can enhance not only the CO_2 injection capacity but also the saline water production capacity. The effect of the number of production wells on the injection capacity and production capacity is more significant than that of well spacing, and the simulation scenario with 2 production wells, one injection well, and a well spacing of 2 km is more reasonable in the demonstration project of Junggar Basin. CO_2-EWR technology can effectively control the evolution of the reservoir pressure and offset the sharp increase in reservoir pressure caused by CO_2 injection and the sharp decrease of reservoir pressure caused by saline production. The main controlling factors of pressure evolution at a certain spatial point in a reservoir change with time. The monitoring pressure drops at the beginning and is controlled by the extraction of water. Subsequently, the injection of CO_2 plays a dominant role in the increase of reservoir pressure. Overall, the results of analysis provide a guide and reference for the CO_2-EWR site selection, as well as the practical placement of wells.

1. Introduction

CO_2 geological storage (CGS) in deep saline aquifers is a potential technology to lower carbon emissions and thereby mitigate global climate change [1]. It has attracted much attention from the Chinese government and enterprises in recent years, particularly in coal-rich regions [2–5]. Traditional CGS projects may cause a series of problems due to the continuous large-scale injection of CO_2 and the reservoir pressure build-up, such as caprock fracturing, upward CO_2

leakage, fault activation, and induced seismicity, all of which will limit the injection capacity of CO_2 and threaten the safety and security of CGS projects [6–8]. The alternative geoengineering approach of CCUS (Carbon Capture, Utilization, and Storage) technology [9–12] is an attractive and potentially viable way to significantly reduce anthropogenic carbon emissions with the benefit of economically productive activities [13].

CGS combined with enhanced water recovery (CO_2-EWR) technology is proposed to make up for the

shortcomings of the traditional CCS technology [14–21]. Compared with traditional deep saline aquifer CGS projects, CO_2-EWR not only can mitigate the excessive build-up of reservoir pressure by a reasonable engineering design of the extraction wells to improve the capability of the injected CO_2 but also produce deep saline water that can be used for industrial or agricultural utilizations after a treatment to effectively alleviate water shortage in arid areas [14, 18].

Davidson et al. [22] suggested that future constraints on CCS deployment are likely to be necessary in areas that have a significant potential demand for deep geologic CO_2 storage and in areas that are already experiencing water stress. To reduce risks associated with the overpressure in the reservoir and to increase the capacity of saline water production and CO_2 storage, Kobos et al. [14] developed a methodology of combining thermal power plants, CO_2 storage in deep saline aquifers and extraction of saline waters. They indicated that injection-induced overpressure particularly in the near-well regions can be relieved by producing water from dedicated water production wells and that the treated saline waters can be used as cooling water for power plants [14, 23], but the adverse consequences are the associated higher costs of the intervention operations [24]. The brine extraction combined with CO_2 injection could effectively reduce the reservoir pressure, and the amount of CO_2 dissolved in the brine will increase significantly due to the extraction of saline water, thereby improving the security of CO_2 storage [25–27].

A series of mathematical/numerical models have been developed to find out the relationship between the reservoir pressure evolution and the process of CO_2 injection or brine extraction. Buscheck et al. [18] introduced active CO_2 reservoir management (ACRM) to prove that brine extraction can reduce pressure build-up and increase storage capacity. The concept of "impact-driven pressure management (IDPM)" suggests that strategic well placement and optimization of extraction may allow for a significant reduction in the saline water production volumes [28]. Li et al. [16] primarily studied the influence of well arrangements and formation parameters on the reservoir pressure evolution by a 3D standard numerical model in the Junggar Basin. Then, the optimizer combining the genetic algorithm and TOUGH2 (GA-TOUGH2) is used to achieve both the maximum efficiency of water production and the maximum capacity of CO_2 storage, taking into account the safety of CGS [19], following the work of Li et al. [16].

Generally, researches about CO_2-EWR are now in the stage of theoretical study, and only one actual project, the Gorgon Project in Australia [29, 30], has been implemented throughout the entire world. How to reasonably optimize the arrangement of the production wells to achieve the trade-off between the safety of CO_2 geological storage and the largest utilization of deep saline water, as well as a strategy of reservoir pressure control, must be studied in an actual CO_2-EWR project. Li et al. [16] and Liu et al. [19] have performed some numerical simulations, whereby the reservoir properties were assumed to be isotropic without considering the heterogeneity in actual conditions, and the range of their models was small with a coarse resolution of each individual grid block. Moreover, the assumption of the closed surrounding boundaries deviates from reality and had a great negative impact on the modeling results.

The impact of the number of production wells and the well spacing on the enhanced efficiency of CO_2 storage and saline production, as well as the key parameters controlling reservoir pressure evolution over time, need to be studied further. Based upon the geological and hydrogeological conditions of the CO_2-EWR test site in the eastern Junggar Basin of China, a series of 3D injection-extraction models with fully coupled wellbores and reservoirs were established to simulate the process of CO_2-EWR over a long period of time. The evolution of the reservoir pressure and the enhanced efficiency of CO_2 storage and saline water production were evaluated. The results of analysis can provide significant information for the actual operation of a CO_2-EWR project.

2. Geology and Reservoir Characterization

The Junggar Basin, located in the northern part of the Xinjiang Uygur Autonomous Region in western China, has the greatest early opportunity for CO_2-EWR or storage of a large volume of carbon emissions in deep saline aquifers with a suitable geology. The water shortage is very serious in the eastern part of the basin, where it is the most enriched area of coal resources in Xinjiang. There are more than sixty coal chemical enterprises in this area, which have exacerbated the crisis of CO_2 emissions and water shortage [31]. The CO_2-EWR test site is situated in the Fukang depression of the Junggar Basin with gentle formations, and the dip angle is approximately five degrees from southwest to northeast.

One deep hole in the site was used for the prefeasibility study of the CO_2-EWR technology. According to the well logging data and drilling data of the existing wells, three reservoir intervals without faults had been perforated between the depths of 1945.5 and 2994 m to carry out CO_2-EWR research. The three perforated intervals are all sandstone aquifers developed in the Cretaceous Donggou Formation and Lian-Sheng Formation, as shown in Figure 1.

The second perforated interval, with a depth of 2241.9-2267.5 m, is employed for the current simulation study based on the pumping tests. The porosity and permeability of the reservoir were determined through the geological investigation and sample analysis (Figure 2), and we assumed that each layer was isotropic.

The variation of porosity and permeability is caused by the periodicity of strata formation sedimentation. The middle part of the strata (high permeability and porosity) and the overlying and underlying layers (low permeability and porosity) form a closed reservoir system where CO_2 can be safely sealed.

3. Simulation Approach

3.1. Simulation Tool. The simulations in the paper were carried out using the well-known multiphase flow solver TOUGH2-MP/ECO2N code [32–35], the parallel version
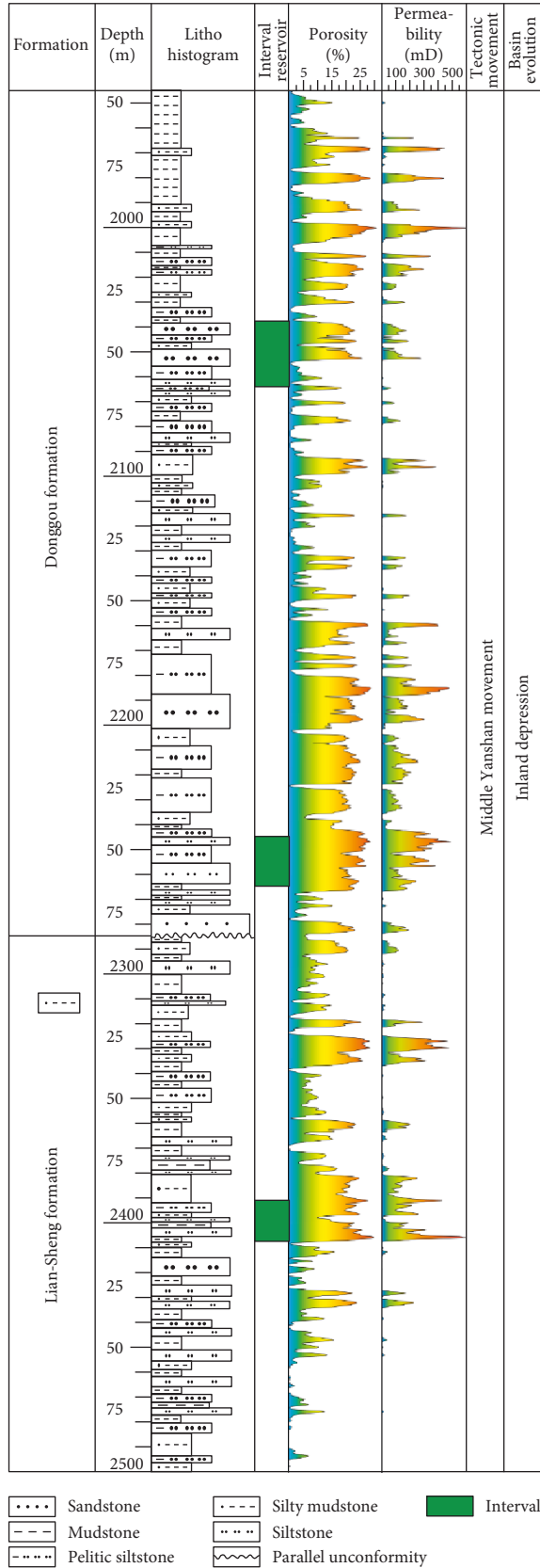
FIGURE 1: Stratigraphic structure characteristics of the study area (the blue color represents lower porosity and permeability, and the orange color represents higher porosity and permeability).

of a fully coupled wellbore-reservoir simulator [36–38] with the fluid property module "ECO2N," which was designed for applications to CO_2 geologic sequestration in deep saline aquifers.

The model domain was constructed using the preprocessing interface software TOUGHVISUAL [39, 40], which was developed for the pretreatment and postprocessing of TOUGH family codes. The friendly interface software can easily create regular or irregular grids, based on the characterizations of geological conceptual models.

3.2. Simulation Scenarios. The number (n) of production wells and the distance (d) between wells may have various impacts on CO_2 migration and reservoir pressure evolution. We designed several simulation scenarios (Table 1) corresponding to the main concerns of evaluating the impacts of the number of production wells and the well spacing on the enhanced efficiency of CO_2 storage and saline water production, as well as the key parameters controlling reservoir pressure evolution over time.

The arrangements of the number of production wells and well spacing refer to the previous research results [41, 42].

3.3. Grid Subdivision. Based on the actual geological conditions of drilling data and geophysical exploration data, a 3D numerical model of the target strata of the CO_2-EWR test site was constructed (Figure 3). The depths of the top and bottom layers of the real target reservoir were 2241.9 m and 2267.5 m, respectively, with a total thickness of 25.6 m. In order to reduce the influence of lateral boundary on the simulation results, the model domains in the X and Y directions were both 20 km.

In view of the model precision of the evaluation and the calculation capability of the computer, a model mesh with an irregular nonequidistant grid subdivision was adopted on the horizontal plane. Each column of well elements was connected to 32 columns of rock elements surrounding the well. A radially discretized submesh was generated with the number of grid units increasing with the distance to the injection/extraction well. The vertical meshes were strictly divided based on the lithology characteristics of the existing well. A total of 18 geological strata were assigned to the 18 grid layers with an average thickness of approximately 1 m. The entire 3D mesh consisted of 23,949 grid blocks for the base-case model with one injection well and one pumping well, and the distance between wells was 2 km (Figure 3).

Figure 4 shows the different 3D grids for the different simulation scenarios. Figures 4(a) and 4(b) represent the sole CO_2 injection and the sole water production scenarios, respectively. Figures 4(c)–4(e) show the scenarios with one injection well and one pumping well, of which the distances between the two wells were 1 km, 3 km, and 5 km, respectively. As shown in Figures 4(f) and 4(g), there were two or four production wells around one injection well with fixed distance between wells of 2 km. The number of model elements is different due to the arrangement of production wells (Table 1).
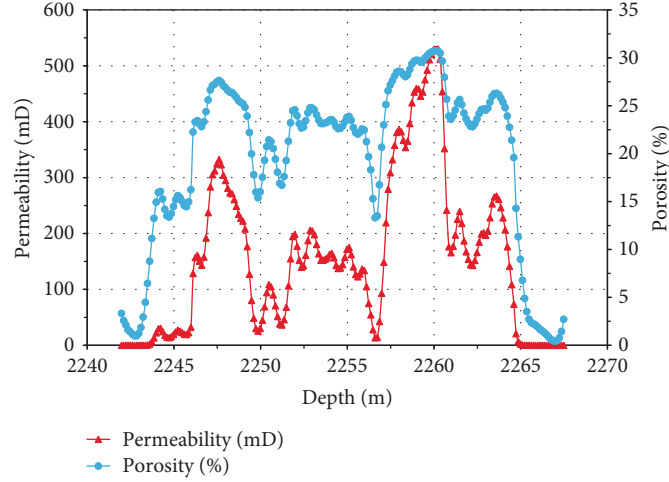
FIGURE 2: Porosity and permeability of the reservoir formations according to borehole logging data.

TABLE 1: Detailed information of different simulation scenarios.

Scenarios	Number of injection wells	Number of production wells	Distance d between wells (km)	Number of model elements
Base case	1	1	2	23,949
Case 1	1	0	/	29,721
Case 2	0	1	/	29,721
Case 3	1	1	1	22,905
Case 4	1	1	3	24,273
Case 5	1	1	5	24,813
Case 6	1	2	2	33,837
Case 7	1	4	2	53,577

3.4. Boundary and Initial Conditions. Based on previous numerical works [43, 44], the Dirichlet boundary conditions were preferred for the lateral boundaries (far enough) with a constant pressure and temperature. The upper and bottom boundaries of the reservoir were assumed to be impermeable due to the great thickness and low permeability of the overlying and underlying layers.

The wellbore was treated as an inner boundary (pressure boundary) rather than a flux boundary because it is a more reliable and efficient way to inject CO_2 in the wellhead of the injection well by the pressure boundary [45, 46], and the same was done for the production well. In addition, the injection pressure at the wellhead was specified as 7 MPa for the supercritical condition of CO_2 [47]. The pressure perturbation due to water extraction should not exceed the fracture pressure of the strata [48, 49], so the bottom hole flowing pressure in the production well was fixed at 7.28 MPa, which is 30% of the reservoir hydrostatic pressure.

The reservoir was initially filled with only saline water with a salinity of 4.32% (mass fraction) according to the pumping tests in the existing well. The initial reservoir pressures and temperature were determined with the monitoring data of the well (Table 2). As mentioned above, we treated the wellbore as a pressure boundary, and the injection pressure at the wellhead was also specified as a constant 7 MPa in previous studies, with the CO_2 gas at saturation and zero salinity [46].

4. Results and Discussion

4.1. The Shut-In Time for Different Scenarios. The postprocessing cost of the extracted saline water will be very expensive if the content of CO_2 in the production stream is too high, which will greatly increase the production cost of enterprises. Hence, a well shut-in time is proposed when the CO_2 content in the production stream is higher than 10%, and the simulations are terminated [19]. For the base-case CO_2-EWR scenario, the well shut-in time is 3.95 years.

As shown in Figure 5, the time required for CO_2 to migrate from the injection well to the production well varies. With the increase in the well spacing between the production well and injection well, the shut-in time increases gradually, and the shut-in time decreases gradually with the increase in the number of production wells. However, the number of production wells has little effect on the shut-in time compared with the well spacing.

After analyzing the shut-in time of each scenario, the effects of CO_2 injection combined with saline water production on CO_2 spatial migration, CO_2 injection and saline water production capacity, and the evolution of reservoir pressure are analyzed in the following section.

4.2. CO_2 Migration in Reservoirs. When the supercritical CO_2 migrates to the production well and reaches a certain concentration (Sg = 0.1), the spatial distribution of CO_2 in the model of CO_2-EWR is obviously different from that of single CO_2 injection, as shown in Figures 6 and 7. Considering the symmetry of the CO_2 spatial distribution, we only analyzed the spatial distribution of CO_2 in the *X-Z* plane ($Y = 0$ m) near the injection well.

4.2.1. Effect of the Well Spacing on CO_2 Migration. Figures 6(b), 6(d), 6(f), and 6(h) show the distribution of
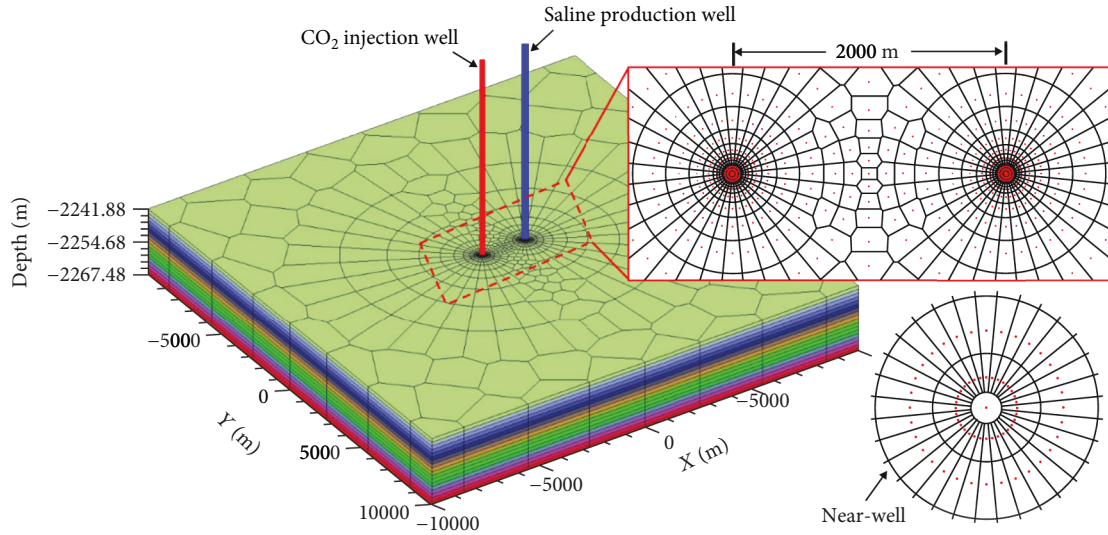
FIGURE 3: The 3D grid of the CO_2-EWR modeling area (base case).

supercritical CO_2 in the CO_2-EWR model at the end of the simulation when the well spacing was 1 km, 2 km, 3 km, and 5 km, respectively, in comparison to the spatial distribution of CO_2 at the same time in the solo CO_2 injection model, as shown in Figures 6(a), 6(c), 6(e), and 6(g). During the injection period, there is a single-phase region of the supercritical CO_2 near the injection well, and the saturation of the supercritical CO_2 decreases gradually with the increasing distance from the injection well in one model. Because of the obvious pore-permeability heterogeneity in the vertical direction, the mudstone layer with relatively low permeability divides CO_2 into several areas vertically, so the spatial distribution of CO_2 is obviously different in the vertical direction. The roof of the reservoir is mudstone with very low permeability, which can effectively prevent CO_2 from migrating to adjacent aquifers, and this improves the safety of CO_2 geological storage.

The placement of production wells makes it easier for CO_2 to migrate towards the wells, resulting in the asymmetric distribution of CO_2 on both sides of the injection well. At the end of the simulation in the CO_2-EWR model, the supercritical CO_2 on the right side of the injection well had already migrated to the production well with a very high saturation (the maximum CO_2 migration distances were 1 km, 2 km, 3 km, and 5 km, respectively). However, the maximum CO_2 migration distances on the left side of the injection well were 584 m, 1230 m, 1896 m, and 2962 m, respectively.

In the solo CO_2 injection model, the spatial distribution of the supercritical CO_2 on both sides of the injection well was symmetrical, and the migration distance was small. Compared with the CO_2-EWR models at the same time, the maximum CO_2 migration distances were 449 m, 1020 m, 1614 m, and 2790 m, respectively, which were not only smaller than the maximum migration distance of the supercritical CO_2 but also smaller than the CO_2 migration distance on the left side of the injection well. The preferential lateral migration of CO_2 was due to the release of reservoir pressure by the saline water production.

4.2.2. Effect of the Number of Production Wells on CO_2 Migration. Figures 7(b), 7(d), and 7(f) show the spatial distribution of supercritical CO_2 in the CO_2-EWR model with 1, 2, and 4 production wells (well spacing of 2 km) at the end of the simulation, in comparison to the spatial distribution of CO_2 at the same time in the solo CO_2 injection model, as shown in Figures 7(a), 7(c), and 7(e).

As shown in Figure 7, the spatial distribution of CO_2 in the CO_2-EWR model with different numbers of production wells was basically similar, the maximum migration distance of CO_2 was 2 km, and CO_2 had migrated to the production wells. In the solo CO_2 injection model, the maximum migration distances of CO_2 were 1020 m, 992 m, and 910 m, respectively, at the same time.

The results of the influence of the well spacing and the number of production wells on CO_2 migration show that the well spacing has a significant effect on the shut-in time, so the maximum migration distance of CO_2 varies greatly. In contrast, the number of production wells has little effect on the shut-in time, so the maximum migration distance of CO_2 has little effect. Compared with traditional CO_2 geological storage technology, the arrangement of production wells can promote the horizontal migration of CO_2, thereby reducing the accumulation of CO_2 concentration and pressure near the injection wells, which can significantly reduce the risk of CO_2 leakage from the reservoir.

4.3. Enhanced Efficiency of the Injection and Production Capacity. In the traditional CCS storage process, the reservoir pressure build-up may limit the injection capacity of CO_2 due to the continuous large-scale injection of CO_2. The placement of saline water production wells at a certain distance from the injection wells can effectively release reservoir pressure and thus may improve the injection efficiency of CO_2. At the same time, CO_2 injection may offset the reservoir pressure reduction caused by solo saline water production, where water is extremely needed and groundwater exploitation is essential. At the same time, this can improve the efficiency
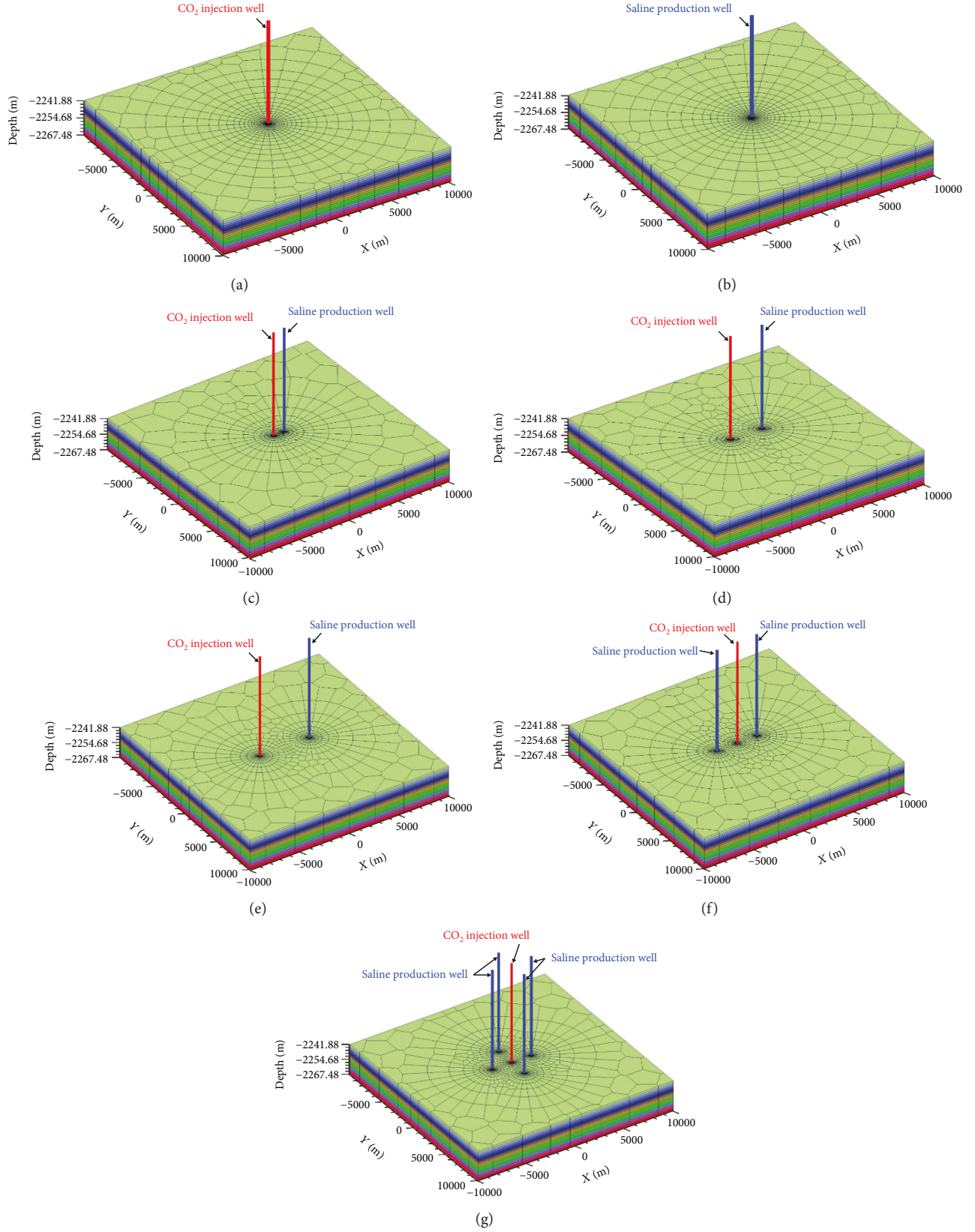
(a)

(b)

(c)

(d)

(e)

(f)

(g)

FIGURE 4: The 3D grid for the simulation scenarios. (a) Sole CO_2 injection. (b) Sole water production. (c) 1 injection well and 1 production well with the well spacing of 1 km. (d) 1 injection well and 1 production well with the well spacing of 3 km. (e) 1 injection well and 1 production well with the well spacing of 5 km. (f) 1 injection well and 2 production wells with the well spacing of 2 km. (g) 1 injection well and 4 production wells with the well spacing of 2 km.

TABLE 2: Geometric and hydrogeological specifications for the simulation.

Reservoir	
Thickness	25.60 m
Porosity	Figure 2
Permeability	Figure 2
Rock grain density	2650 kg/m^3
Rock specific heat	920 J/kg/°C
Rock thermal conductivity	2.51 W/m/°C
Initial conditions	
Reservoir fluid	Saline water (salinity of 4.32%)
Reservoir temperature	63.00°C
Average reservoir pressure	21.89 MPa
Initial CO_2 saturation	0
Wellbores	
Diameter	0.20 m
Roughness	0.046 mm
Heat conductivity	2.51 W/m/°C
Inclination of wells	Vertical
Injection-production distance	Table 1
Injection pressure (wellhead)	7.00 MPa
Production pressure (downhole)	7.28 MPa
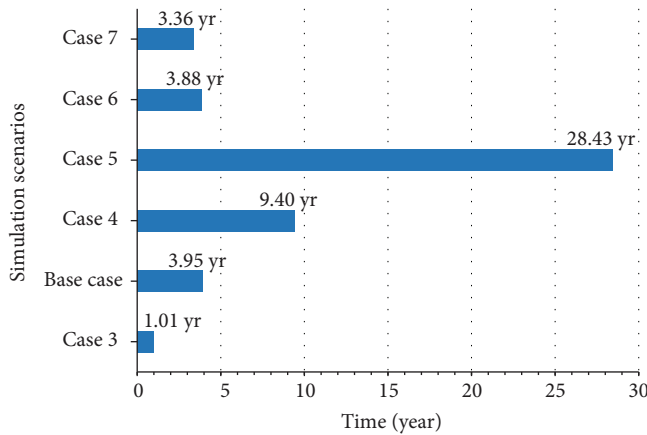
FIGURE 5: The shut-in time for different CO_2-EWR simulation scenarios (year).

of saline water production, and the produced saline water can be used for local industry and agriculture after treatment.

Then we need to quantitatively evaluate the influence of the well spacing and the number of production wells on the CO_2 injection capacity and saline water production capacity during the process of CO_2-EWR.

4.3.1. Influence of the Placement of the Production Wells on the Injection and Production Capacity. When there is only one production well, the influence of the well spacing on the CO_2 injection capacity and saline water production capacity is shown in Figure 8.

Figures 8(a) and 8(c) show that the injection rate increases rapidly at the beginning of the CO_2 injection period and that the injection rate can be stabilized after a long simulation time. During the simulation period, the injection capacity of CO_2 is linearly related to the time. In the solo CO_2 injection model, the injection rate was 19.52 kg/s, and the amount of injected CO_2 was 2.32 million tons after 4 years. In the CO_2-EWR model with a well spacing of 1 km, the injection rate under the same wellhead pressure was 35.32 kg/s at a time of 1.01 years when the simulation was terminated because the CO_2 content in the production stream was higher than 10%, the injection rate was increased by 101.48% compared with the solo CO_2 injection model at the same time, and the CO_2 injection amount was approximately 1 million tons. When the well spacing was 2 km, the injection rate of CO_2 was 33.90 kg/s, 73.85% higher than the solo injection model, and 3.78 million tons of CO_2 was injected after 3.95 years. When the well spacing was 3 km and 5 km, the injection rate was 28.46 kg/s and 25.51 kg/s and had increased by 45.80% and 30.69% after 4 years, respectively. After 9.4 years and 28.43 years, the CO_2 injection amounts were 8.40 million tons and 24.92 million tons, respectively.

The influence of well spacing on the CO_2 injection rate and amount is significant. The smaller the well spacing, the greater the CO_2 injection rate due to the more obvious influence of the production wells on the reservoir pressure. However, with the increasing well spacing, the longer the simulation period and the larger the cumulative injection amount.

As shown in Figures 8(b) and 8(d), at the early stage of saline production, the production rate will reach a peak, and then, the production rate will continue to decline, finally reaching a stable stage in a short period of time. The effect of the well spacing on the production rate and amount was not obvious. In the solo saline water production model, the stable rate was 53.88 kg/s, and the total amount of produced saline water could be 6.86 million tons in four years. When the well spacing was 1 km in the CO_2-EWR model, the increase for pressure in the reservoir system caused by CO_2 injection will transmit to the production well in a short time. As a result, more saline water is displaced to the production well by the high-pressure CO_2, and the saline water production rate will be higher than others with larger well spacing, so the production rate was 66.29 kg/s at 1.01 years, which is 22.60% higher than that of the solo saline water production model at the same time, and the amount of saline water production was 2.15 million tons. When the well spacing is 2 km, the production rate was 62.39 kg/s, an increase of 15.79% compared with the solo production model, and the production amount increased to 7.60 million tons after 3.95 years. When the well spacing is 3 km and 5 km, the production rate was approximately 56.17 kg/s and 55.09 kg/s after 4 years and had only increased by 4.25% and 2.25%, which is close to the solo saline water production rate at the same time. However, after 9.40 years for the 3 km well spacing and 28.43 years for the 5 km well spacing, the saline water production amounts were approximately 16.69 million tons and 49.57 million tons, respectively.
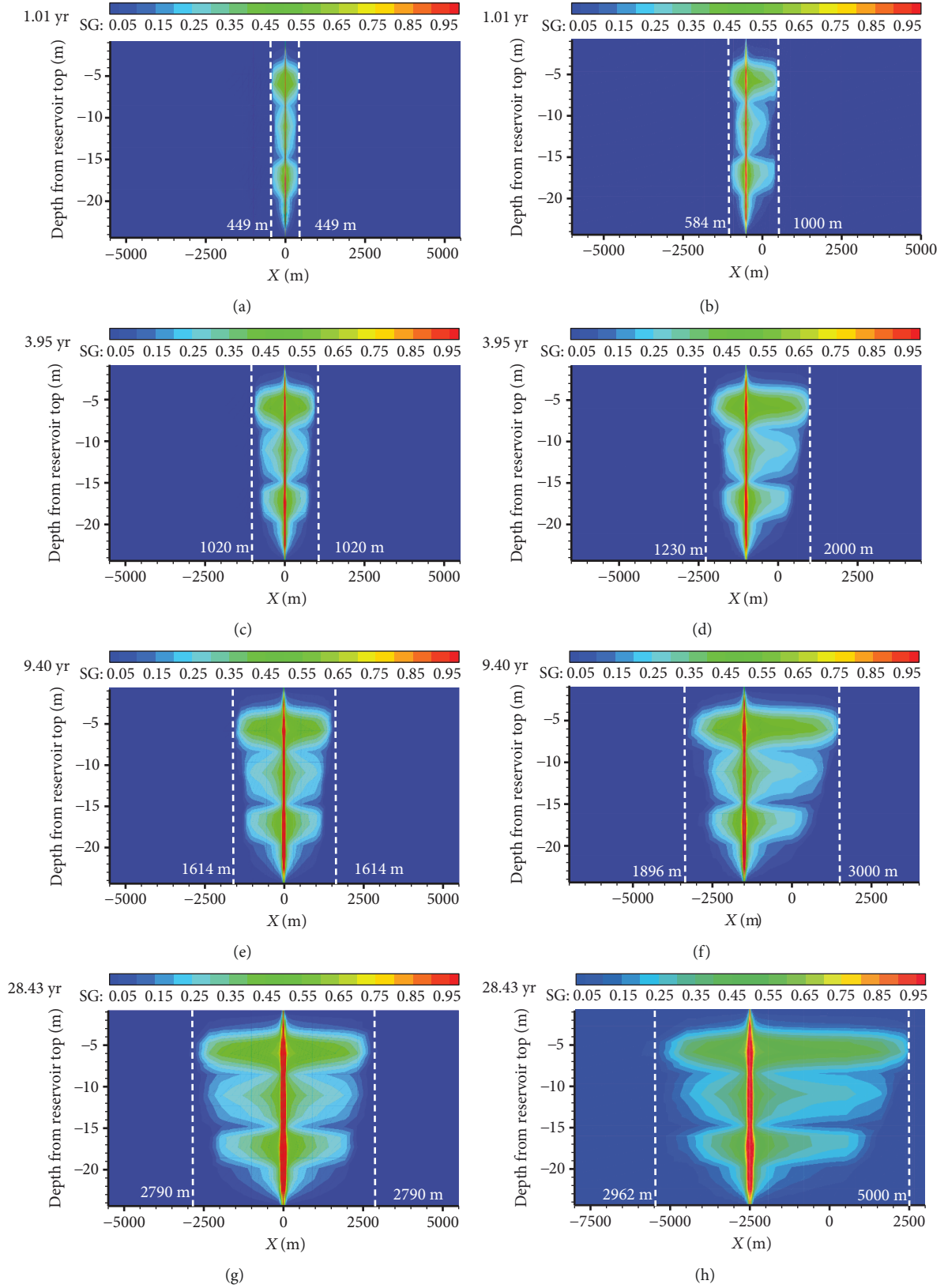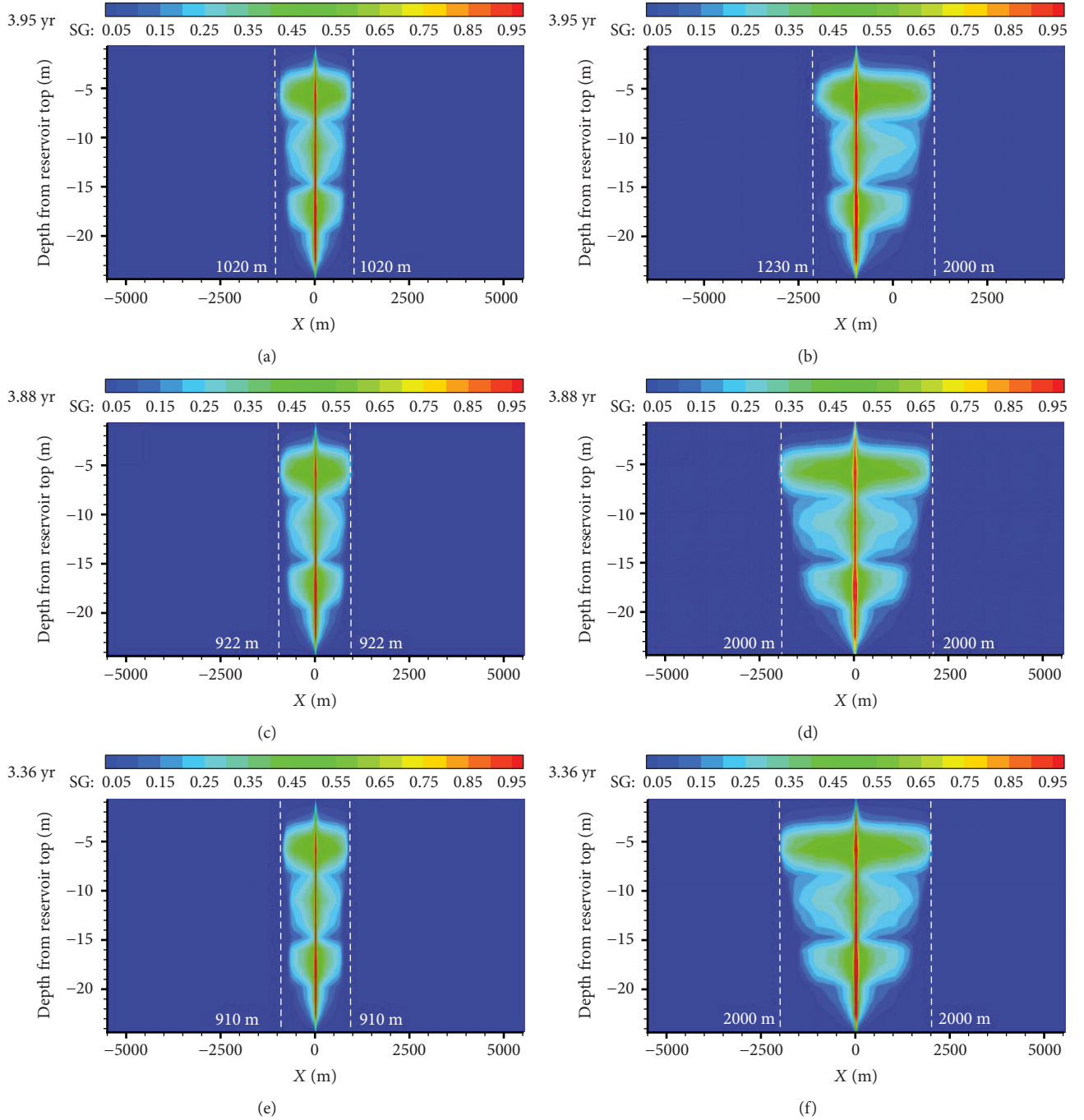
FIGURE 6: Spatial distribution of the supercritical CO_2 at the end of the simulation in different scenarios (analysis of the well spacing). (a) Sole CO_2 injection at 1.01 years. (b) The well spacing of 1 km at 1.01 years. (c) Sole CO_2 injection at 3.95 years.(d) The well spacing of 2 km at 3.95 years. (e) Sole CO_2 injection at 9.40 years. (f) The well spacing of 3 km at 9.40 years. (g) Sole CO_2 injection at 28.43 years. (h) The well spacing of 5 km at 28.43 years.

FIGURE 7: Spatial distribution of the supercritical CO_2 at the end of the simulation in different scenarios (analysis of number of the production wells). (a) Sole CO_2 injection at 3.95 years. (b) One production well at 3.95 years. (c) Sole CO_2 injection at 3.88 years. (d) Two production wells at 3.88 years. (e) Sole CO_2 injection at 3.36 years. (f) Four production wells at 3.36 years.

Hence, the effect of well spacing on the enhancement of the saline water production rate is not as significant as that of the CO_2 injection rate during the process of CO_2-EWR. When the well spacing increases to a certain distance (for example, 3 km in this study), the enhancement effect of CO_2-EWR on the rate of saline water production is negligible, but the amount of saline water production increases significantly with increasing well spacing due to the increase in the simulation period.

Figure 9 shows the effect of different numbers of production wells on the CO_2 injection and production capacity when the well spacing was fixed to 2 km.

As shown in Figures 9(a) and 9(c), the number of production wells had a great influence on both the CO_2 injection rate and the injection amount. When there was no production well, the injection rate of CO_2 was only 19.52 kg/s, and the cumulative injection amount was 2.32 million tons after 4 years. When there was one production well, the injection
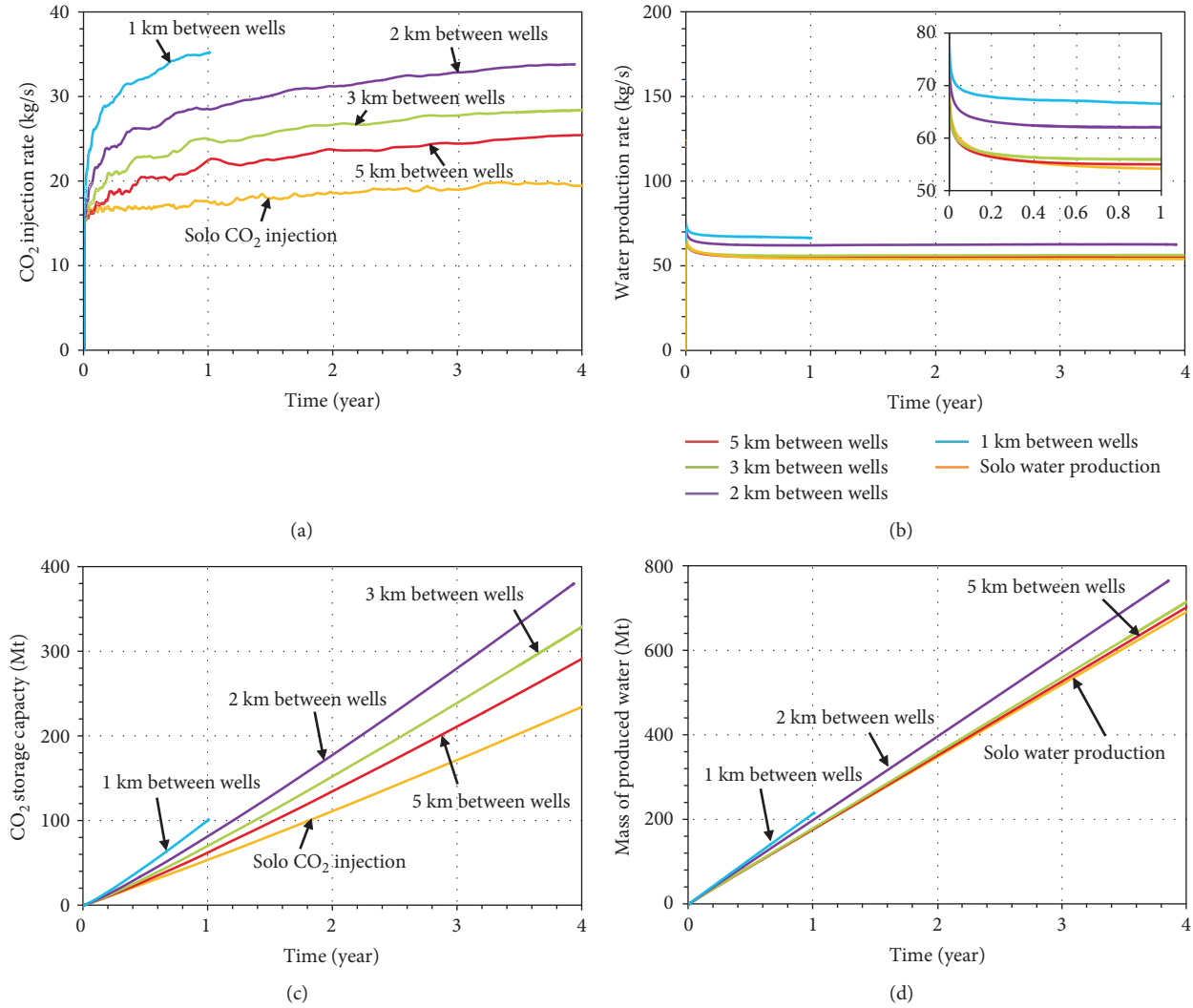
(a)

(b)

(c)

(d)

FIGURE 8: The effect of the well spacing on the CO_2 injection and saline water production capacity. (a, b) Injection and production rates. (c, d) Injection and production amounts.

rate of CO_2 was 33.90 kg/s at the end of 3.95 years, which is 73.85% higher than that of the single CO_2 injection model at the same time, and the cumulative injection amount was 3.77 million tons. When there were two production wells, the injection rate was 45.25 kg/s at 3.88 years, which was 1.30 times the solo injection rate with the CO_2 injection amount totaling 4.69 million tons. At the end of 3.36 years in the model with 4 production wells, the injection rate of CO_2 was 65.48 kg/s, an increase of 229.54%, and the total CO_2 injection amount reached 5.95 million tons. The increase in the number of production wells had a positive effect on the efficiency of CO_2 injection.

It can be seen from Figure 9(b) that the rate of saline water production in each well declines rapidly at the beginning of the simulation during the process of CO_2-EWR, but with the passing of simulated time, the rate rises slightly. Because the process of CO_2 injection can lead to an increase in the reservoir pressure, this will offset the pressure decrease caused by saline water extraction near the production wells, and the injected CO_2 can promote the migration of saline

water to the production wells, thereby replenishing the saline water in the production area.

When the spacing between the injection and production wells is fixed, the stable production rate of saline water in each production well decreases gradually with the increase in the number of production wells, as shown in Figure 9(b). In the solo production model, the stable production rate was 53.88 kg/s, with a total amount of saline water production of 68.62 million tons after 4 years. The production rate was 62.39 kg/s, an increase of 15.79%, when there was one production well at the time of 3.95 years, and the amount of production was 7.60 million tons. In the model with two production wells, the steady rate in each production well was 55.58 kg/s after 3.88 years, only increasing by 3.16%. The total amount of saline water production in the two wells was 13.59 million tons. When the number of production wells increased to 4, the rate of saline water production in each well was 50.32 kg/s at the end of 3.36 years, which was lower than that of the solo saline water production rate. When the number of production wells increases, the saline
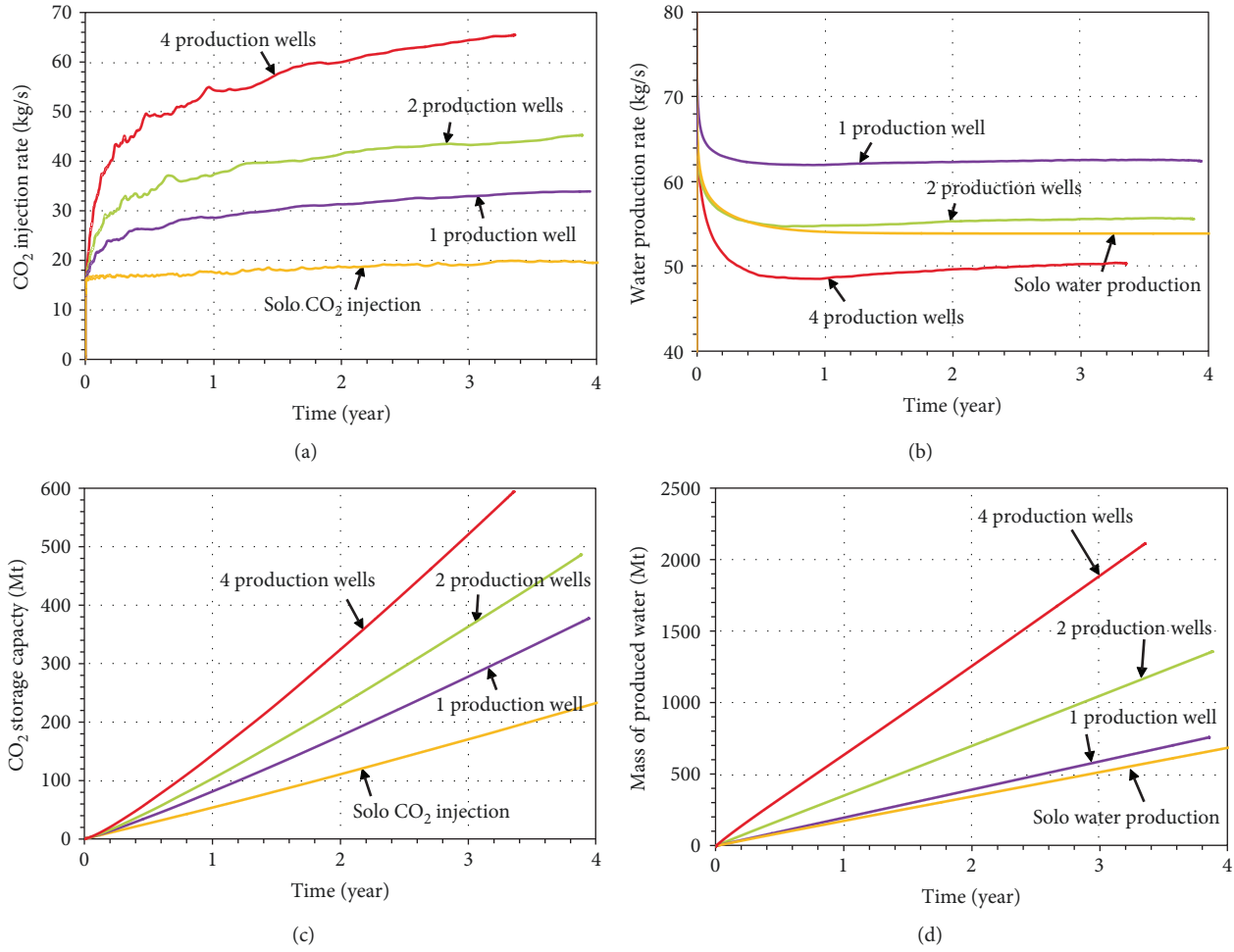
(a)

(b)

(c)

(d)

FIGURE 9: The effect of the number of production wells on the CO_2 injection and saline water production capacity. (a, b) Injection and production rates. (c, d) Injection and production amounts.

water in the reservoir is extracted in a short time, and the rate of saline water recharge in the production area cannot meet the demand for short-term extraction. Although the rate of saline water production in each well decreases with the increase in the number of production wells, the total rate of all wells was still very large, and the total amount of saline water production of four wells was 21.14 million tons in 3.36 years (Figure 9(d)).

4.3.2. Optimization Scenario for the CO_2-EWR Project in the Junggar Basin. To optimize the arrangement of production wells, we evaluated the effects of the well spacing and the number of production wells on the annual CO_2 injection amount and annual saline water production amount (Figures 10 and 11). Firstly, the suitable well spacing for the site was applied (Figures 10 and 11), then the preferred number of production wells was determined (Figures 10–12). Finally, we came to the reasonable optimization scenario for the CO_2-EWR project in the Junggar Basin of China.

Figure 10 shows the effect of the well spacing and the number of production wells on the annual CO_2 injection amount. In the solo CO_2 injection model and the CO_2-EWR
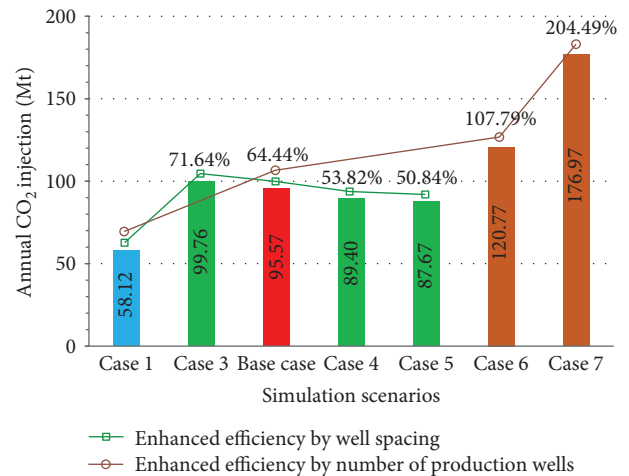

FIGURE 10: Influence of the arrangement of the production wells on the CO_2 injection capacity.

model with one production well with different well spacing, the annual CO_2 injection amount is less than 1 million tons. With the increase in well spacing, the enhancement efficiency
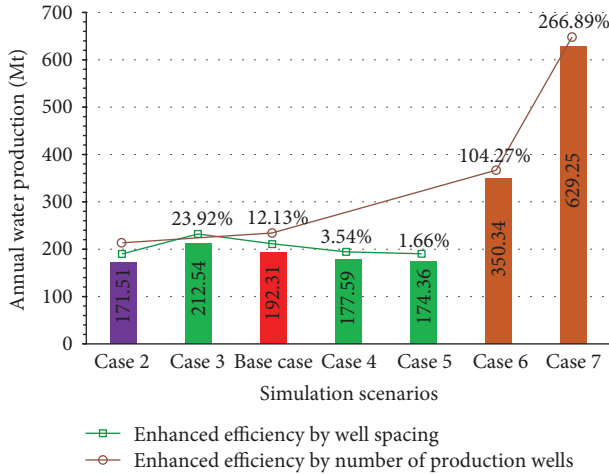
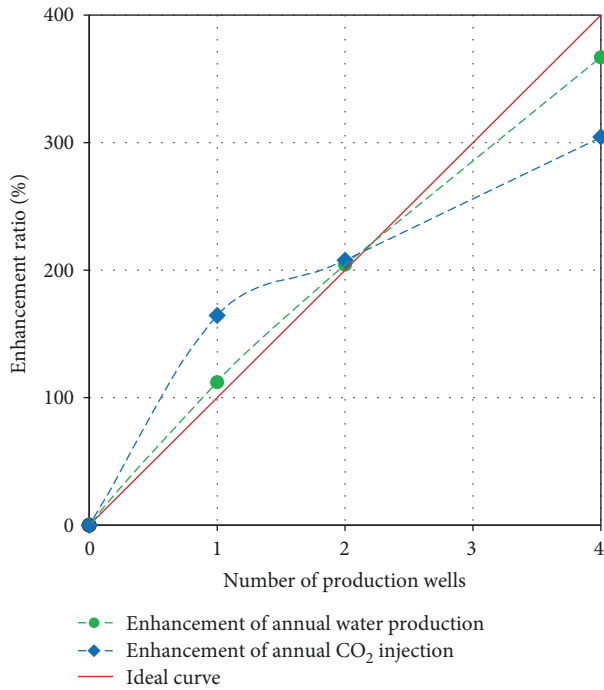FIGURE 11: Influence of the placement of the production wells on the saline water production capacity.

FIGURE 12: The enhanced efficiency of the number of production wells on the CO_2 injection and saline water production capacity.
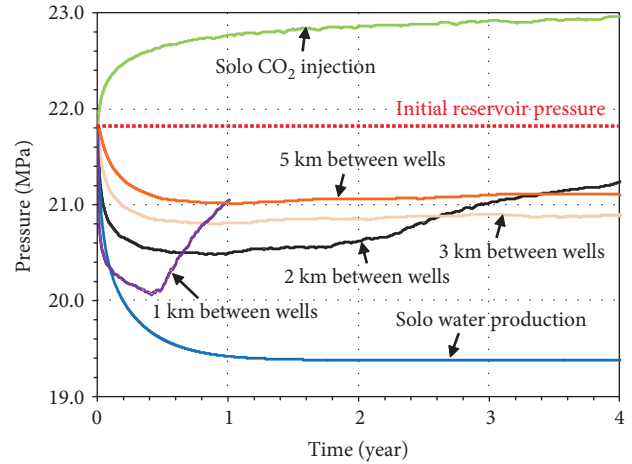

FIGURE 13: The pressure evolution curve at the monitoring point under different well distance layout conditions.

between 12.13% and 23.92%. The enhancement efficiency of annual saline water production is less than 3.54% when the well spacing is greater than 3 km. The number of production wells has a significant influence on the annual saline water production amount. Although the production rate in a single well decreases with the increase in the number of production wells (Figure 9(b)), the total production amount is still very large due to the large number of production wells. The annual operating time of coal-fired power generating units is approximately 5,500 hours, and the installed water consumption rate is approximately $0.6 \, m^3/(s \cdot GW)$ in the study area at present [50]. In this study, when there are two production wells, the annual saline water production capacity is 3.03 million tons, which can meet the annual water consumption demand of a thermal power plant with an installed capacity of 300 MW.

The above analyses of the influence of the placement of production wells on the CO_2 injection and saline water production capacity indicate that the CO_2 injection and saline water production capacity decrease with increasing well spacing. Therefore, the smaller well spacing can meet the needs of massive CO_2 injection and salt water production, but the simulation period is too short to generate enough economic benefits when the well spacing is less than 1 km (Figures 8(c) and 8(d)). When the well spacing is greater than 3 km, the enhancement efficiency of CO_2-EWR technology on the CO_2 injection and saline water production is not obvious, so a 2 km well spacing is more suitable for our study area.

As shown in Figures 10 and 11, the effect of the number of production wells on the injection capacity and production capacity is more significant than that of well spacing, but the increase in production wells will correspondingly increase the project cost, so it is necessary to analyze the enhanced efficiency of production wells. From Figure 12, it can be seen that the enhancement efficiency of CO_2 injection and saline water production declines when there are more than two production wells. The enhancement efficiency is higher than the theoretical enhancement efficiency when the number of production wells is one and two. To maximize the enhancement efficiency of CO_2 injection and saline water production

of CO_2 injection is gradually weakened, and the influence of the well spacing on the CO_2 injection amount is not obvious. When the number of production wells increases to 2 and 4, the annual CO_2 injection amount increases to more than 1 million tons, and the increase in the number of production wells has a significant effect on the enhancement of CO_2 injection capacity.

The influence of the well spacing and the number of production wells on the annual saline water production amount is shown in Figure 11. The well spacing has little effect on the enhancement efficiency of saline water production. When the well spacing is within 2 km, the enhancement efficiency is
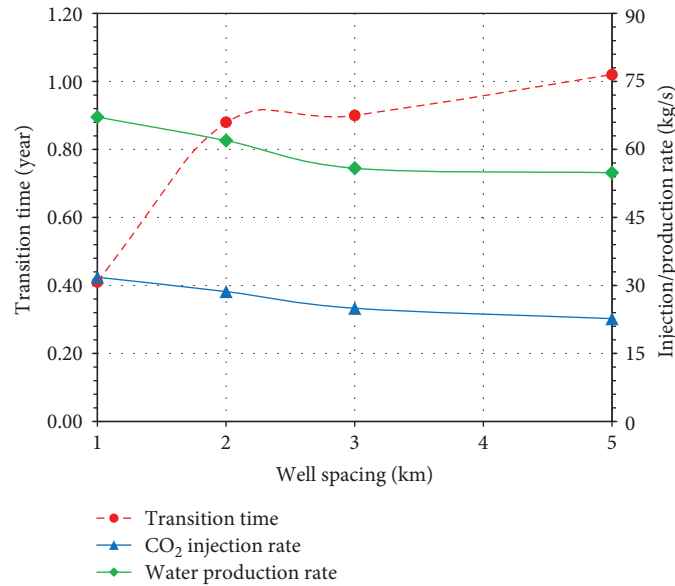
FIGURE 14: Influence of the well spacing on the transition time point, injection rate, and production rate.

and to obtain the greatest economic benefits, the scenario with two production wells is more reasonable.

In summary, the implementation of CO_2 injection combined with saline water production technology has a great enhancement efficiency for both CO_2 injection and saline water production capacity. CO_2-EWR technology can not only achieve the goal of lowering carbon emissions to mitigate global climate change but also produce enough water resources to meet the local water demand. The actual site simulation of the Junggar Basin shows that the simulation scenarios with 2 production wells with one injection well and a 2 km well spacing are more reasonable.

4.4. Controlling Factors of the Reservoir Pressure Evolution. The pressure in the reservoir is monitored, and the pressure monitoring point is in the middle of the injection well and the production well, $z = -7$ m below the caprock. The initial reservoir pressure of the monitoring point is 21.82 MPa. The analysis of the temporal variation of the pressure and the controlling factors of reservoir pressure evolution at this point for different simulation scenarios can provide guidance for reservoir safety evaluations and reservoir protection strategies for CO_2-EWR project design and operation.

As shown in Figure 13, the reservoir pressure increases rapidly in the solo CO_2 injection model at the early stage. After 1 year, the reservoir pressure increases slowly and finally stabilizes after 3 years. The stable pressure was 22.93 MPa, an increase of 1.11 MPa compared with the initial pressure. At the same time, the reservoir pressure decreased sharply because of the saline water production in the solo water production model, and the reservoir pressure reached a stable state after 2 years with a pressure of 19.38 MPa, a decrease of 2.44 MPa.

In the CO_2-EWR model, the pressure of the monitoring point dropped notably because of the saline water production during the early simulation stage. Then, the pressure rose slowly due to the continuous CO_2 injection. When there is only one production well with a well spacing of 1 km, the reservoir pressure decreased to 20.07 MPa after 0.41 years. As the injection-production well spacing was small, the CO_2 injection affected the monitoring point earlier, and the reservoir pressure rapidly rose to 21.05 MPa at 1.01 years. The evolution of the pressure at the monitoring point was mainly controlled by the water production during the early stage lasting 0.41 years. Then, the pressure increased, and the controlling factors changed to the CO_2 injection process. When the well spacing was 2 km, the pressure at the monitoring point decreased to the lowest value of 20.48 MPa at 0.88 years, then rose slowly to 20.54 MPa after 4 years. When the well spacing was 3 km and 5 km, the reservoir pressure decreased to a stable value of 20.80 MPa and 21.01 MPa, respectively. The pressure in the reservoir was mainly controlled by saline water production during the early stage, and the pressure at the monitoring point decreased rapidly. However, when the well spacing was less than 3 km, the monitoring point was close to the injection well and the CO_2 injection process quickly affected the monitoring point as time passed, resulting in a significant rise in the pressure. Finally, the reservoir pressure could be restored to the initial pressure of the formation.

Figure 14 indicates the influence of the well spacing on the transition time point, injection rate, and production rate; the transition time point indicates the transformation moment of the main controlling factors on the pressure evolution. The transition time point increased gradually with the well spacing, and the CO_2 injection rate and saline water production rate gradually decreased at this time point. When the well spacing was greater than 2 km, the decreasing trend of the injection and production rate was weakened, and the increasing trend of the transition time point was weakened accordingly. The pressure evolution at the monitoring point was controlled by the saline water production before the transition time point
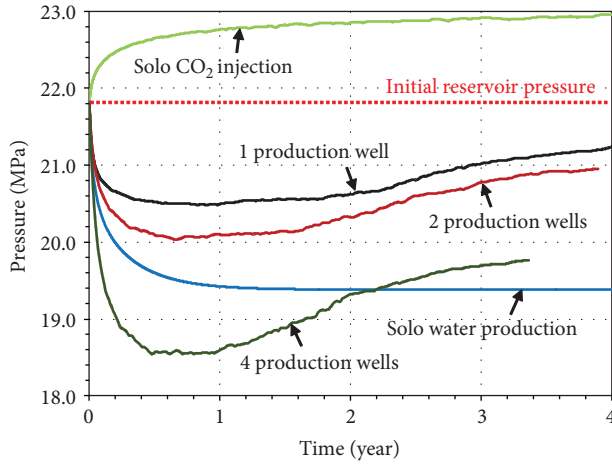
FIGURE 15: The pressure evolution curve at the monitoring point under different numbers of production well conditions.

and then controlled by CO_2 injection. The enhancement efficiency of CO_2 injection and saline water production by the CO_2-EWR technology was weakened (Figure 8) as the distance between the monitoring point to the injection or production well increased with the increase in well spacing, and the increasing trend of the transition time point also slowed down.

Figure 15 shows the temporal variation of the pressure at the monitoring point under different numbers of production well conditions. Although CO_2 injection can raise the reservoir pressure slightly, it still dropped rapidly with the increasing number of production wells as time passed. The pressure at the monitoring point dropped to 18.54 MPa after 0.48 years when there were four production wells in the reservoir, which was 3.28 MPa lower than the initial reservoir pressure, and it did not reach the critical fracture pressure [51]. Then, the pressure rose gradually due to CO_2 injection, and the pressure was restored to 19.76 MPa after 3.36 years, which was still lower than the original hydrostatic pressure of the reservoir; hence, the threat to the mechanical properties and to the security of the reservoir was weakened. When there were one or two production wells, the pressure at the monitoring point decreased slightly, with a maximum decrease of 1.76 MPa. In the later stage, the pressure was mainly controlled by CO_2 injection. Although the initial reservoir pressure could not be restored to the initial pressure, it was significantly improved compared with the scenario of solo water production.

As shown in Figure 16, when the well spacing was fixed to 2 km, the transition time point of the main controlling factors on the monitoring pressure was progressively advanced, and the CO_2 injection rate increased gradually with the number of production wells. At the same time, the water production rate of each well decreased gradually. The transition time point was reduced to 0.48 years when there were four production wells, and the CO_2 injection rate and water production rate were 49.53 kg/s and 48.98 kg/s, respectively. Then, the CO_2 injection rate increased gradually, but the production rate decreased gradually (Figure 9(a)). Therefore, the

pressure evolution at the monitoring point was mainly controlled by the CO_2 injection in this stage, so the pressure rose gradually (Figure 15).

To explore the relationship between the main controlling factors of the pressure evolution at the monitoring point and the injection and production rate, we analyzed the temporal variation of the pressure and of the injection and production rate in the base-case model with one production well and one injection well, with a well spacing of 2 km, as shown in Figure 17. At the beginning of the simulation, the rate of saline water production was much higher than the CO_2 injection rate, and the pressure at the monitoring point decreased rapidly. Then, the water production rate decreased as the CO_2 injection rate increased, and the trend of the pressure decrease was weakened. The main controlling factor of the pressure in this stage was the process of saline water production, and the reservoir pressure remained stable for some time. As the simulation continued, the production rate reached a stable level, while the CO_2 injection rate still increased slowly, and the pressure increased gradually. The main controlling factor of the pressure in this stage was CO_2 injection.

The variation tendency of the pressure at the monitoring point is the same in Figure 17 as for the other simulation scenarios during the process of CO_2-EWR. The main controlling factors of the pressure evolution at a certain spatial point in the reservoir change with time. The transition time point is affected by the well spacing, the number of production wells, and the spatial position in the reservoir. When the monitoring point is in the middle of the injection well and the production well as is the case in our model with one production well and one injection well and a well spacing of 2 km, the pressure evolution is mainly controlled by the water production in the first 0.88 years; then, the main controlling factor of the pressure is the process of CO_2 injection.

Moreover, CO_2-EWR technology can effectively control the reservoir pressure and avoid the drastic increase in reservoir pressure caused by traditional CO_2 geological storage and the drastic decrease of reservoir pressure caused by solo saline water extraction. Therefore, it can become an effective CCUS technology.

5. Conclusions

Based upon the geological and hydrogeological conditions of the CO_2-EWR test site in the eastern Junggar Basin, a series of 3D injection-extraction models with fully coupled wellbores and reservoirs were established to evaluate the effect of the number of production wells and the well spacing on the enhanced efficiency of CO_2 storage and saline production, as well as the key parameters controlling the reservoir pressure evolution, and the following conclusions were obtained:

(1) CO_2-EWR technology can promote the horizontal migration of CO_2 during the process of CGS, thereby reducing the accumulation of the CO_2 concentration and pressure near the injection wells, which can
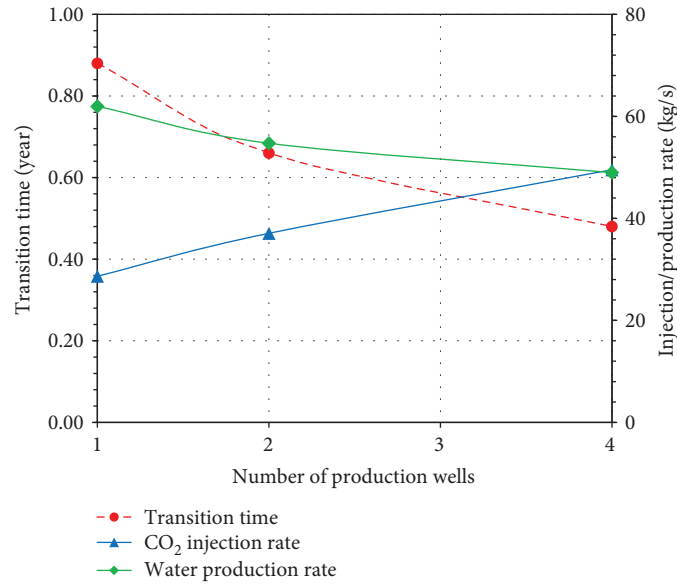
FIGURE 16: Influence of the number of production wells on the transition time point, injection rate, and production rate.
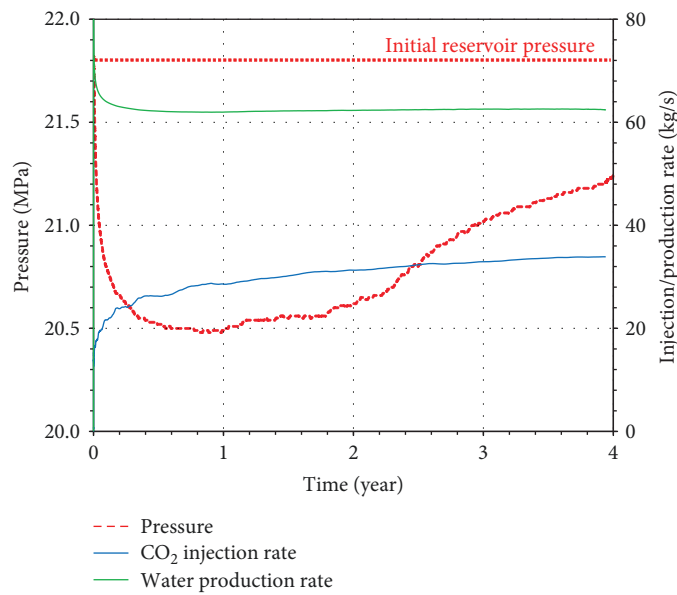

FIGURE 17: Temporal variation of the monitoring pressure and the injection and production rate.

significantly reduce the risk of CO_2 leakage along the injection wellbore

(2) A smaller spacing between the injection and production wells and a larger number of production wells can enhance not only the CO_2 injection capacity but also the saline water production capacity. However, the effect of the number of production wells on the injection and production capacity is more significant than that of the well spacing

(3) The actual site simulation of the Junggar Basin shows that the simulation scenario with 2 production wells, one injection well, and a well spacing of 2 km is the most reasonable, and the annual production capacity

can meet the water requirements of a 300 MW thermal power plant

(4) During the CO_2-EWR process, the main controlling factors of the pressure evolution at a certain spatial point in a reservoir change with time. The transition time point is affected by the well spacing, the number of production wells, and the spatial position in the reservoir

(5) CO_2-EWR technology can effectively control the evolution of the reservoir pressure and offset the sharp increase in reservoir pressure caused by CO_2 injection and the sharp decrease of reservoir pressure caused by saline production. It can avoid possible

reservoir damage during the implementation of a CGS project and ensure the reservoir stability and safety of the project

The implementation of a CO_2-EWR project plays an active role in the eastern Junggar Basin, which can not only achieve the goal of lowering carbon emissions to mitigate global climate change but also produce enough water resources to meet the local water demand. The potential of CO_2 injection and saline water production can be significant. The sensitivity analysis of the reservoir parameters and the influence of geochemistry on CO_2 migration and the capacity of CO_2 injection and saline water production need to be studied further.

Data Availability

The data used to support the findings of this study are available from the corresponding author upon request.

Conflicts of Interest

The authors declare that they have no conflicts of interest.

Acknowledgments

References

[1] IPCC, *The Physical Science Basis. Fourth Assessment Report*, Cambridge University Press, Cambridge, UK, 2007.

[2] D. Best and B. Beck, "Status of CCS development in China," *Energy Procedia*, vol. 4, pp. 6141–6147, 2011.

[3] W. Chen and R. Xu, "Clean coal technology development in China," *Energy Policy*, vol. 38, no. 5, pp. 2123–2130, 2010.

[4] The Administrative Center for China's Agenda 21, *Technology Roadmap Study on Carbon Capture, Utilization and Storage in China*, Science Press, Beijing, China, 2012.

[5] X. Zhang, J. L. Fan, and Y. M. Wei, "Technology roadmap study on carbon capture, utilization and storage in China," *Energy Policy*, vol. 59, pp. 536–550, 2013.

[6] X. Lei, S. Ma, W. Chen, C. Pang, J. Zeng, and B. Jiang, "A detailed view of the injection-induced seismicity in a natural gas reservoir in Zigong, southwestern Sichuan Basin, China," *Journal of Geophysical Research: Solid Earth*, vol. 118, no. 8, pp. 4296–4311, 2013.

[7] J. Birkholzer, Q. Zhou, and C. Tsang, "Large-scale impact of CO_2 storage in deep saline aquifers: a sensitivity study on pressure response in stratified systems," *International Journal of Greenhouse Gas Control*, vol. 3, no. 2, pp. 181–194, 2009.

[8] IEAGHG, *Potential Impacts on Groundwater Resources of CO2 Storage*, IEAGHG, Cheltenham, UK, 2011.

[9] F. Quattrocchi, E. Boschi, A. Spena, M. Buttinelli, B. Cantucci, and M. Procesi, "Synergic and conflicting issues in planning underground use to produce energy in densely populated countries, as Italy: geological storage of CO_2, natural gas, geothermics and nuclear waste disposal," *Applied Energy*, vol. 101, pp. 393–412, 2013.

[10] M. M. F. Hasan, E. L. First, F. Boukouvala, and C. A. Floudas, "A multi-scale framework for CO_2 capture, utilization, and sequestration: CCUS and CCU," *Computers & Chemical Engineering*, vol. 81, pp. 2–21, 2015.

[11] D. A. Wood, "Carbon dioxide (CO_2) handling and carbon capture utilization and sequestration (CCUS) research relevant to natural gas: a collection of published research (2009–2015)," *Journal of Natural Gas Science and Engineering*, vol. 25, pp. A1–A9, 2015.

[12] M. Extavour and P. Bunje, "CCUS: utilizing CO_2 to reduce emissions," *Chemical Engineering Progress*, vol. 112, pp. 52–59, 2016.

[13] J. F. D. Tapia, J. Y. Lee, R. E. H. Ooi, D. C. Y. Foo, and R. R. Tan, "Planning and scheduling of CO_2 capture, utilization and storage (CCUS) operations as a strip packing problem," *Process Safety and Environmental Protection*, vol. 104, pp. 358–372, 2016.

[14] P. H. Kobos, M. A. Cappelle, J. L. Krumhansl, T. A. Dewers, A. Mcnemar, and D. J. Borns, "Combining power plant water needs and carbon dioxide storage using saline formations: implications for carbon dioxide and water management policies," *International Journal of Greenhouse Gas Control*, vol. 5, no. 4, pp. 899–910, 2011.

[15] Q. Li, Y. N. Wei, G. Liu et al., "Feasibility of the combination of CO_2 geological storage and saline water development in sedimentary basins of China," *Energy Procedia*, vol. 37, pp. 4511–4517, 2013.

[16] Q. Li, Y. N. Wei, G. Liu, and Q. Lin, "Combination of CO_2 geological storage with deep saline water recovery in western China: insights from numerical analyses," *Applied Energy*, vol. 116, pp. 101–110, 2014.

[17] Q. Li, Y. N. Wei, G. Liu, and H. Shi, "CO_2-EWR: a cleaner solution for coal chemical industry in China," *Journal of Cleaner Production*, vol. 103, pp. 330–337, 2015.

[18] T. A. Buscheck, Y. Sun, M. Chen et al., "Active CO_2 reservoir management for carbon storage: analysis of operational strategies to relieve pressure buildup and improve injectivity," *International Journal of Greenhouse Gas Control*, vol. 6, pp. 230–245, 2012.

[19] D. Liu, R. Agarwal, and Y. Li, "Numerical simulation and optimization of CO_2-enhanced water recovery by employing a genetic algorithm," *Journal of Cleaner Production*, vol. 133, pp. 994–1007, 2016.

[20] W. L. Bourcier, T. J. Wolery, T. Wolfe, C. Haussmann, T. A. Buscheck, and R. D. Aines, "A preliminary cost and engineering estimate for desalinating produced formation water associated with carbon dioxide capture and storage," *International Journal of Greenhouse Gas Control*, vol. 5, no. 5, pp. 1319–1328, 2011.

[21] R. D. Aines, T. J. Wolery, W. L. Bourcier, T. Wolfe, and C. Hausmann, "Fresh water generation from aquifer-pressured carbon storage: feasibility of treating saline formation waters," *Energy Procedia*, vol. 4, pp. 2269–2276, 2011.

[22] C. L. Davidson, J. J. Dooley, and R. T. Dahowski, "Assessing the impacts of future demand for saline groundwater on commercial deployment of CCS in the United States," *Energy Procedia*, vol. 1, no. 1, pp. 1949–1956, 2009.

[23] P. E. S. Bergmo, A. A. Grimstad, and E. Lindeberg, "Simultaneous CO_2 injection and water production to optimise aquifer storage capacity," *International Journal of Greenhouse Gas Control*, vol. 5, no. 3, pp. 555–564, 2011.

[24] T. le Guénan and J. Rohmer, "Corrective measures based on pressure control strategies for CO_2 geological storage in deep aquifers," *International Journal of Greenhouse Gas Control*, vol. 5, no. 3, pp. 571–578, 2011.

[25] B. Court, K. W. Bandilla, M. A. Celia et al., "Initial evaluation of advantageous synergies associated with simultaneous brine production and CO_2 geological sequestration," *International Journal of Greenhouse Gas Control*, vol. 8, pp. 90–100, 2012.

[26] Y. Li, Q. Fang, Y. Ke, J. Dong, G. Yang, and X. Ma, "Effect of high salinity on CO_2 geological storage: a case study of Qianjiang depression in Jianghan basin," *Earth Science*, vol. 37, pp. 283–288, 2012.

[27] T. Kabera and Y. L. Li, "Injecting CO_2 and pumping out saline formation water simultaneously to control pressure build-up while storing CO_2 in deep saline aquifers," *Defect and Diffusion Forum*, vol. 332, pp. 63–75, 2012.

[28] J. T. Birkholzer, A. Cihan, and Q. Zhou, "Impact-driven pressure management via targeted brine extraction—conceptual studies of CO_2 storage in saline formations," *International Journal of Greenhouse Gas Control*, vol. 7, pp. 168–180, 2012.

[29] M. A. Flett, G. J. Beacher, J. Brantjes et al., "Gorgon Project: subsurface evaluation of carbon dioxide disposal under Barrow Island," *Journal of Petroleum Technology*, vol. 61, pp. 71-72, 2008.

[30] M. Flett, J. Brantjes, R. Gurton, J. Mckenna, T. Tankersley, and M. Trupp, "Subsurface development of CO_2 disposal for the Gorgon Project," *Energy Procedia*, vol. 1, no. 1, pp. 3031–3038, 2009.

[31] J. Zhou, X. Zhuang, A. Alastuey, X. Querol, and J. Li, "Geochemistry and mineralogy of coal in the recently explored Zhundong large coal field in the Junggar basin, Xinjiang province, China," *International Journal of Coal Geology*, vol. 82, no. 1-2, pp. 51–67, 2010.

[32] K. Pruess, "Numerical simulation of CO_2 leakage from a geologic disposal reservoir, including transitions from super- to subcritical conditions, and boiling of liquid CO_2," *SPE Journal*, vol. 9, no. 2, pp. 237–248, 2013.

[33] K. Pruess, *ECO2N: A TOUGH2 Fluid Property Module for Mixtures of Water, NaCl, and CO_2*, Lawrence Berkeley National Laboratory. Earth Sciences Division, Berkeley, CA, USA, 2005.

[34] K. Pruess, C. Oldenburg, and G. Moridis, *TOUGH2 User's Guide, Version 2.0. Report LBNL4 43134, Lawrence Berkeley National Laboratory*, Lawrence Berkeley National Laboratory. Earth Sciences Division, Berkeley, CA, USA, 1999.

[35] K. Zhang, Y. Wu, and K. Pruess, *User's Guide for TOUGH2-MP-A Massively Parallel Version of the TOUGH2 Code*, Lawrence Berkeley National The Laboratory Earth Sciences Division, Berkeley, CA, USA, 2008.

[36] L. Pan, C. M. Oldenburg, Y. Wu, and K. Pruess, *T2Well/E-CO2N Version 1.0: Multiphase and Non-Isothermal Model for Coupled Wellbore-Reservoir Flow of Carbon Dioxide and Variable Salinity Water*, Lawrence Berkeley National Laboratory. Earth Sciences Division, Berkeley, CA, USA, 2011.

[37] L. Pan and C. M. Oldenburg, "T2Well—an integrated wellbore–reservoir simulator," *Computers & Geosciences*, vol. 65, pp. 46–55, 2014.

[38] T. Xu, G. Feng, Z. Hou, H. Tian, Y. Shi, and H. Lei, "Wellbore–reservoir coupled simulation to study thermal and fluid processes in a CO_2-based geothermal system: identifying favorable and unfavorable conditions in comparison with water," *Environmental Earth Sciences*, vol. 73, no. 11, pp. 6797–6813, 2015.

[39] Y. Yang, F. Bu, T. Xu, and F. Wang, "The anisotropy effect on CO_2-water two phase fluid migration-improve the TOUGH2 simulator function," *Journal of Northeastern University*, vol. 35, pp. 1211–1216, 2014.

[40] Y. Yang, T. Xu, F. Wang, H. Lei, G. Jing, and G. Yue, "Toughvisual: a user-friendly pre-processing and post-processing graphical interface for TOUGHREACT," in *Proceedings TOUGH Symposium*, pp. 17–19, Berkeley, CA, USA, 2012.

[41] Q. Fang, *CO_2 Geological Storage Combined with Brine Production in High-Salinity and Low-Permeability Aquifers*, China University of Geosciences, Wuhan, China, 2014.

[42] Z. Dai, R. Middleton, H. Viswanathan et al., "An integrated framework for optimizing CO_2 sequestration and enhanced oil recovery," *Environmental Science & Technology Letters*, vol. 1, no. 1, pp. 49–54, 2013.

[43] F. Bu, T. Xu, F. Wang, Z. Yang, and H. Tian, "Influence of highly permeable faults within a low-porosity and low-permeability reservoir on migration and storage of injected CO_2," *Geofluids*, vol. 16, no. 4, 781 pages, 2016.

[44] F. Wang, J. Jing, Y. Yang et al., "Impacts of injection pressure of a dip-angle sloping strata reservoir with low porosity and permeability on CO_2 injection amount," *Greenhouse Gases: Science and Technology*, vol. 7, no. 1, pp. 92–105, 2017.

[45] C. Li, K. Zhang, Y. Wang, C. Guo, and F. Maggi, "Experimental and numerical analysis of reservoir performance for geological CO_2 storage in the Ordos Basin in China," *International Journal of Greenhouse Gas Control*, vol. 45, pp. 216–232, 2016.

[46] Z. Yang, T. Xu, F. Wang, Y. Yang, X. Li, and N. Zhao, "Impact of inner reservoir faults on migration and storage of injected CO_2," *International Journal of Greenhouse Gas Control*, vol. 72, pp. 14–25, 2018.

[47] K. Pruess and J. Garcia, "Multiphase flow dynamics during CO_2 disposal into saline aquifers," *Environmental Geology*, vol. 42, no. 2-3, pp. 282–295, 2002.

[48] J. B. Walsh, "Effect of pore pressure and confining pressure on fracture permeability," *International Journal of Rock Mechanics and Mining Sciences & Geomechanics Abstracts*, vol. 18, no. 5, pp. 429–435, 1981.

[49] G. R. Johnson and W. H. Cook, "Fracture characteristics of three metals subjected to various strains, strain rates, temperatures and pressures," *Engineering Fracture Mechanics*, vol. 21, no. 1, pp. 31–48, 1985.

[50] M. Han, "Analysis and countermeasures on water consumption in thermal power plants," *Industrial Water Treatment*, vol. 30, pp. 4–7, 2010.

[51] M. K. Hubbert, "Mechanics of hydraulic fracturing," *Developments in Petroleum Science*, vol. 210, pp. 369–390, 1972.